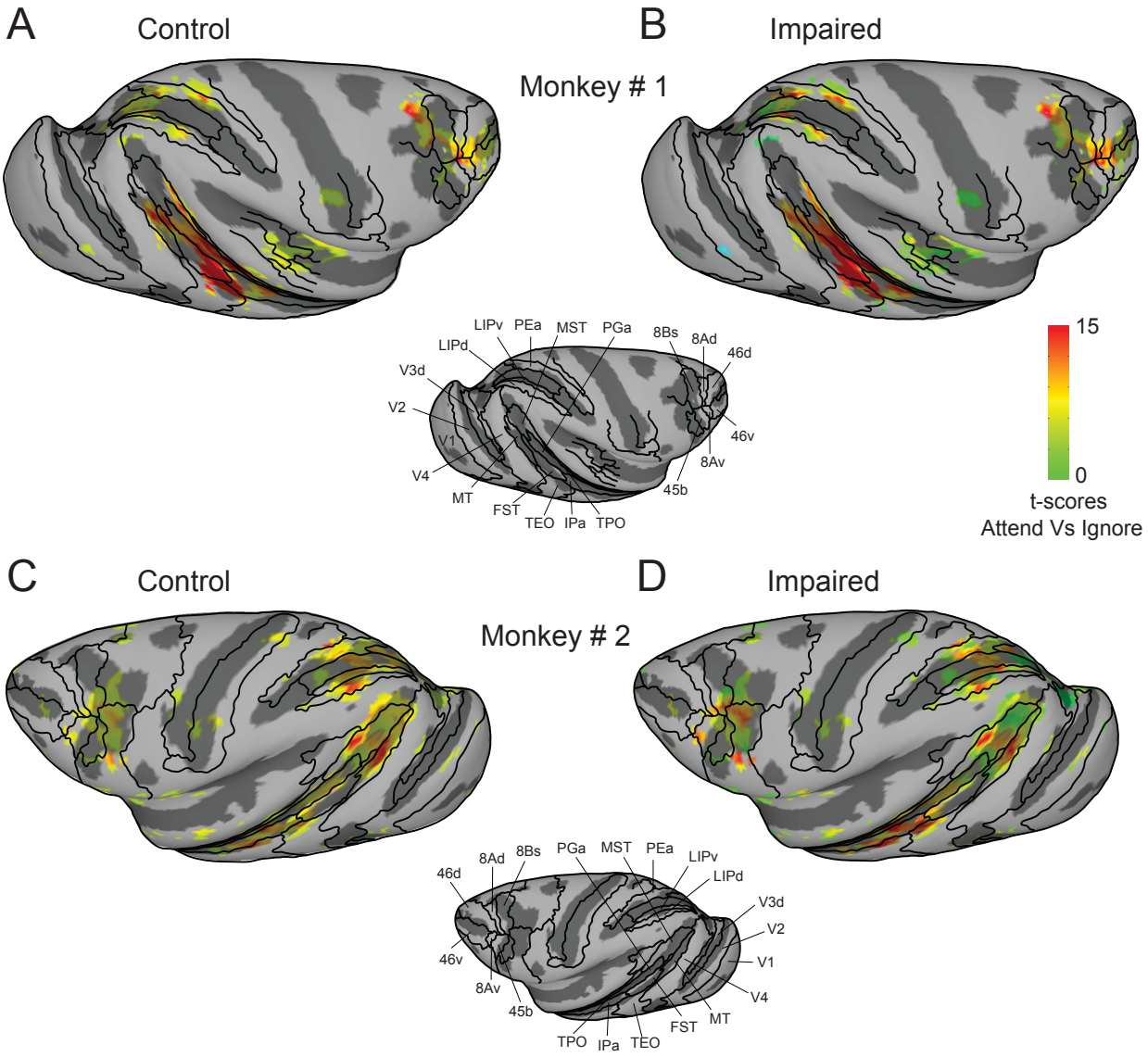

Figure S1. Cortical maps of attention-related modulation in the contralateral hemisphere during control and impaired sessions (related to Figure 2)

(**A,B**) Inflated cortical maps of t-scores showing attention-related modulation in contralateral (right) hemisphere of monkey # 1 during control (**A**) and impaired sessions (**B**). The maps were thresholded during control sessions (**A**) and the modulation for the same voxels is shown during the impaired sessions (**B**).

(**C,D**) Same conventions as (**A,B**) but for monkey # 2.

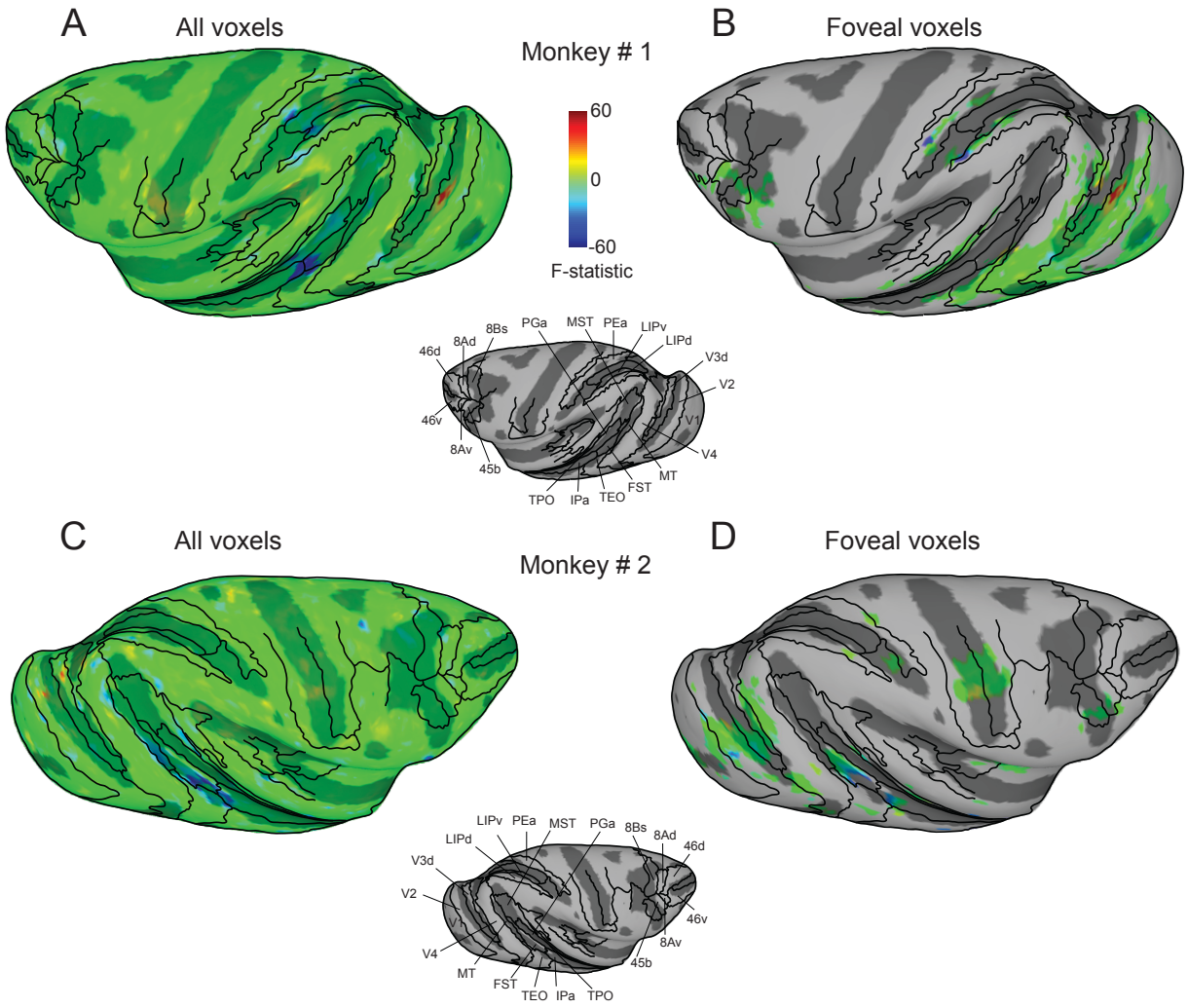

Figure S2. Effect of SC inactivation on all voxels and voxels that map onto foveal locations (related to Figure 3)

Inflated cortical maps of interaction term F-statistic show voxels whose modulation was affected during attention deficits induced by SC inactivation in the ipsilateral hemispheres of both monkeys. The blue color indicates voxels whose modulation was reduced the most during impaired performance and the green colors indicate voxels with no reduction in modulation. (**A,C**) The effect during impaired performance is shown for all voxels in the ipsilateral hemisphere of monkey # 1 (**A**) and monkey # 2 (**C**). (**B,D**) The effect during impaired is shown for voxels that map onto foveal locations in the ipsilateral hemisphere of monkey # 1 (**B**) and monkey # 2 (**D**). Cortical regions corresponding to the fovea were unaffected by SC inactivation; the main effect of SC inactivation was diminished attention-related enhancement in *non-foveal* regions.

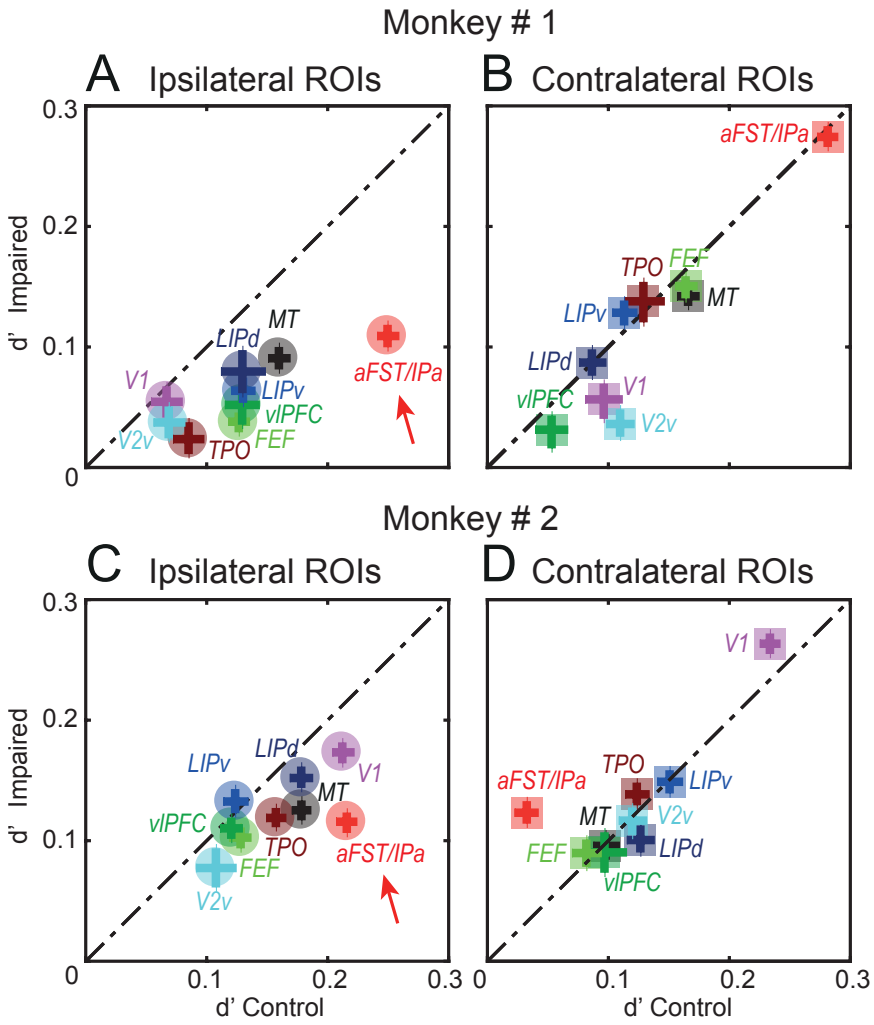

Figure S3. Comparison of the effects of SC inactivation on the attention-related modulations in cortical ROIs (related to Figure 4).

For both monkeys, SC inactivation had the strongest effects on the ipsilateral aFST/IPa region (red arrows). Attention-related modulation during impaired sessions is plotted against the attention-related modulation during control sessions for each ROI in the ipsilateral (**A,C**) and contralateral (**B,D**) hemispheres of both monkeys. In ROIs that lie significantly below the line of identity, attention-related modulation during impaired sessions was significantly reduced compared to the modulation during control. The error bars indicate boot-strapped 95% confidence intervals. Among all ROIs in the ipsilateral hemispheres of monkey #1 (**A**) and monkey #2 (**C**), the aFST/IPa ROI (red symbol and arrows) showed the strongest reduction in modulation and hence lies the furthest from the line of unity slope. In contrast, the aFST/IPa regions in the contralateral hemisphere of monkey #1 (**B**) and monkey #2 (**D**) did not show significant reductions.

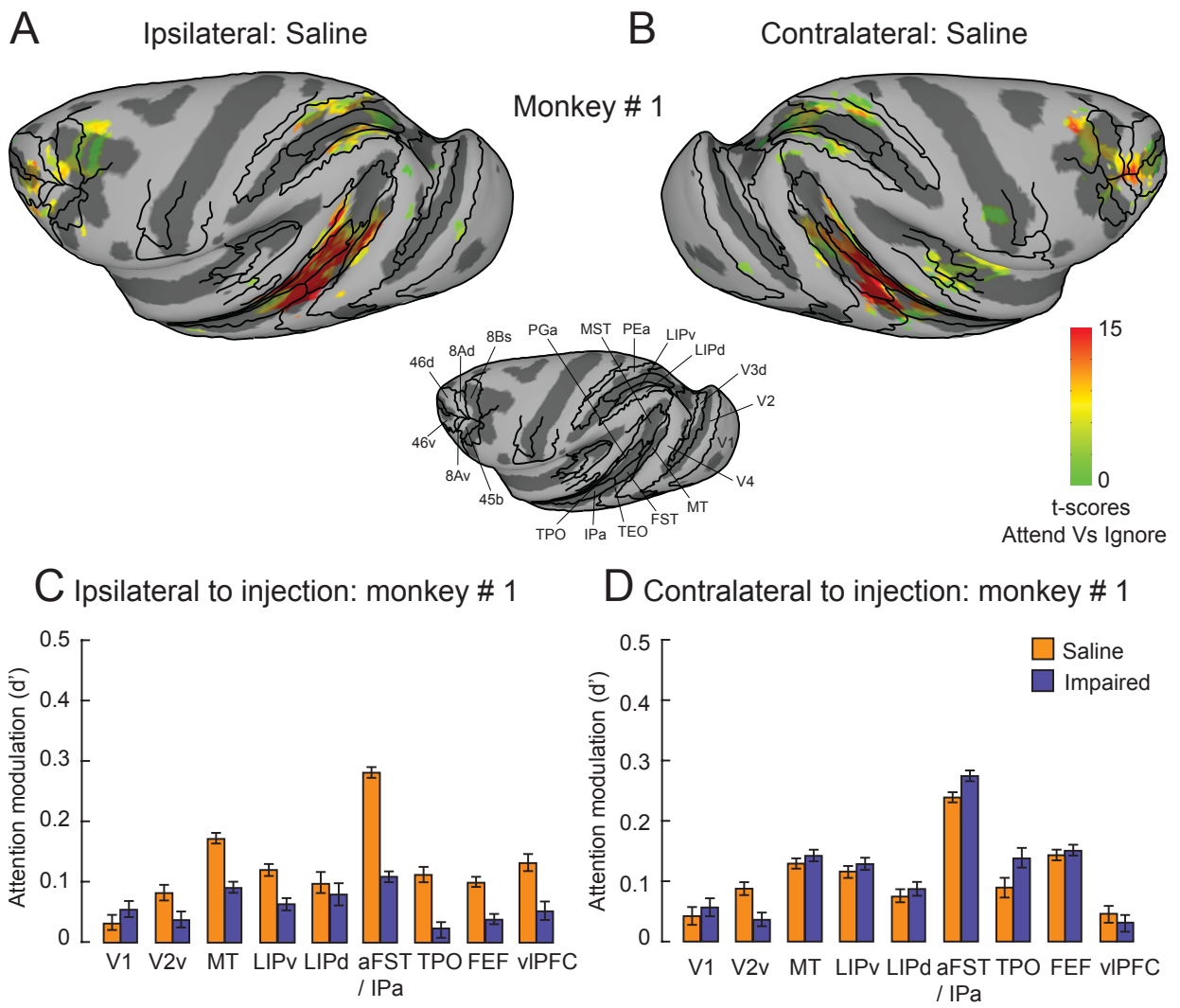

Figure S4. Comparison of attention-related modulation in cortical ROIs between impaired (SC inactivation) and saline sessions (related to Figure 4)

(**A,B**) Inflated cortical maps of t-scores showing attention-related modulation in ipsilateral (**A**) and contralateral (**B**) hemispheres of monkey # 1 during saline injection sessions. The maps were thresholded during control sessions (Figure 2, Figure S1) and the modulation for the same voxels is shown during the saline sessions (**A,B**).

(**C,D**) In the ipsilateral and contralateral ROIs defined based on the attention-related modulation map during control (Figure 2A, Figure S1A), we compared modulation in the same voxels during impaired and saline sessions. The bar plot shows the attention-

related modulation in the ipsilateral (**C**) and contralateral (**D**) ROIs measured as d' during impaired (SC inactivation) and saline sessions. Error bars indicate 95% CI. Again, we found unilateral effects in aFST/lPa, TPO and FEF ROIs consistent with the comparison between control and during SC inactivation. Because the ROIs were independently identified based on the attention-related modulations during control sessions, these results also address the concern that we might have been biased to see reductions in modulation when comparing control and impaired sessions in the ROIs identified from the control sessions.

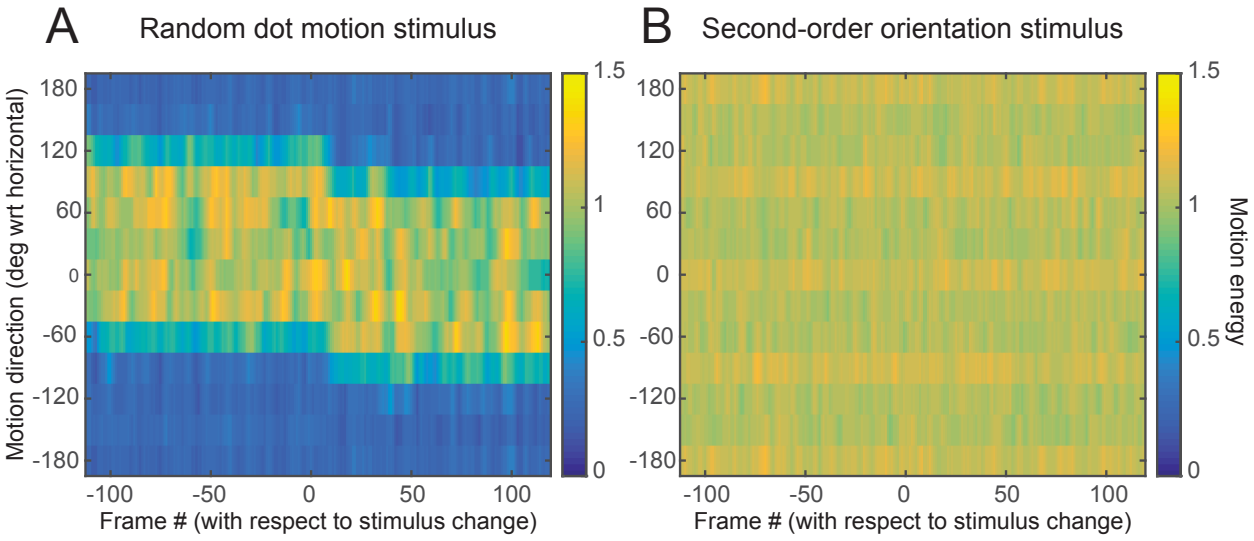

Figure S5. Confirmation that our second-order orientation stimulus was invisible to motion energy filters (related to Figure 5, Video S1 and Video S2).

(**A**) For the random dot motion stimulus (Video S1), the motion energy plot shows a clear peak initially at +30 degrees that then transitions over several frames to a peak at 0 degrees (rightward horizontal motion). (**B**) For the second-order orientation stimulus (Video S2), there is equal activation of all motion energy channels and, in particular, no modulation of motion energy when the contrast modulation is applied (i.e., starting at frame 0).

Motion energy was measured using a previously published motion energy model (*Vision Research* 44:1733-1755, 2004; *J. Vision* 8: 1-14, 2008). The model takes as its input 8-frame sequences and reports the motion energy across 12 equally spaced direction channels and 4 spatial scales. For our measurements, we stepped through the two sample videos provided as Supplemental Information (8-frame snippets in 232 1-frame steps) and measured the average motion energy in each direction channel (averaged over spatial scales). The identical code was applied to both stimulus videos.

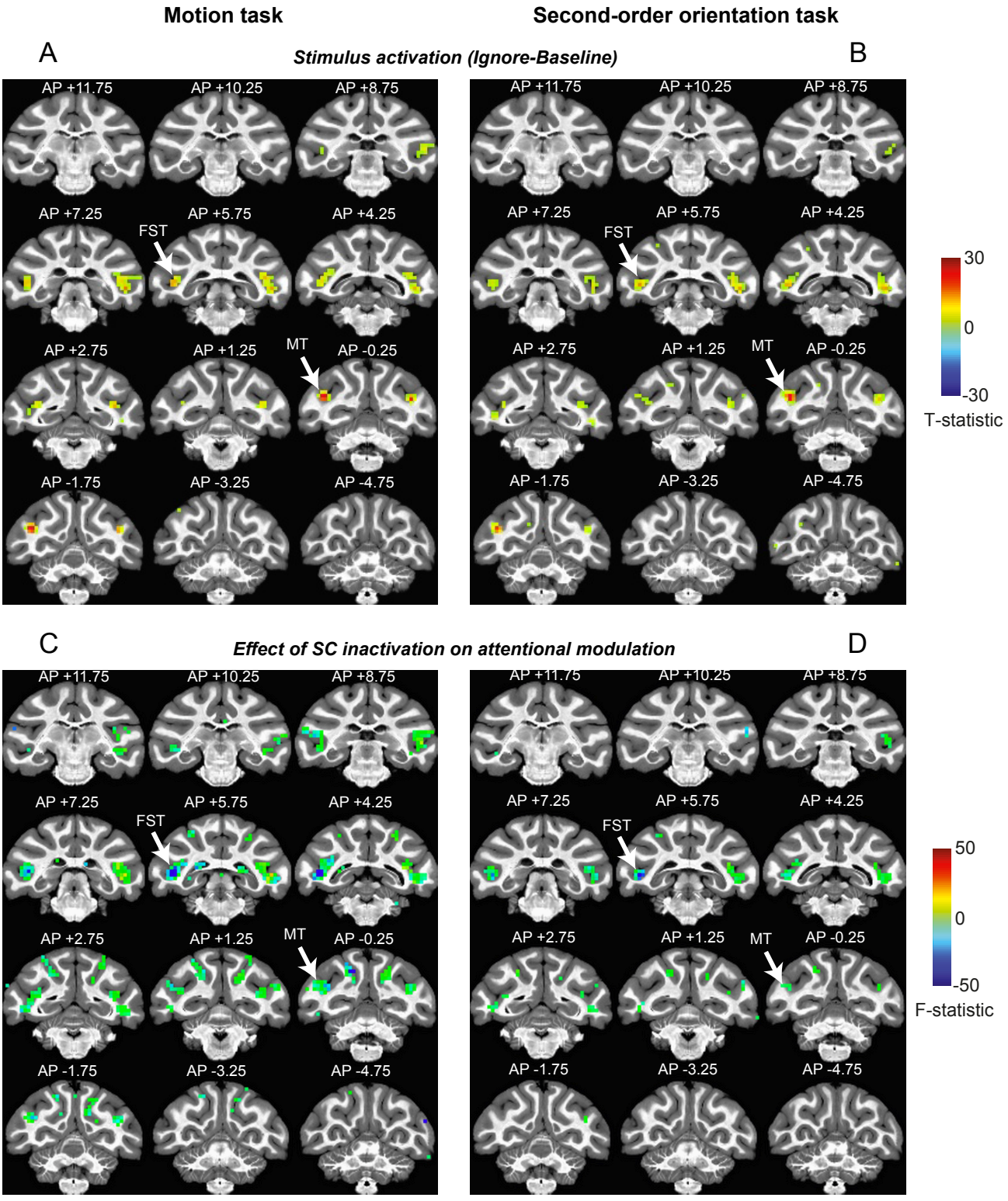

Figure S6. Cortical slices illustrating that peak activations related to the visual stimuli are different from the peak decreases due to SC inactivation (related to Figure 5).

One possibility is that aFST/IPa was most strongly affected during SC inactivation in our experiments simply because it was the region most strongly modulated by the visual stimuli in our tasks; the data presented in this figure rule out this interpretation.
(**A,B**) Mosaic of slices showing the stimulus activations (i.e., Ignore minus Baseline) for the random dot motion stimulus (A) and the second-order orientation stimulus (B). The stimulus activations include aFST/IPa for both stimuli, but aFST/IPa is not the maximum for either the random dot motion or second-order orientation stimulus. The peak stimulus activation in both cases is seen in MT.
(**C,D**) The effect of SC inactivation on attention-related modulation for both visual stimulus for the same mosaic of slices. In both cases the maximum reduction was found in aFST/IPa, even though MT showed stronger stimulus activations. In fact, attention-related modulation in MT for the second-order orientation stimulus was much weaker overall, because unlike the random dot motion stimulus (which contained strong directional motion), the second-order orientation stimulus did not contain a feature to attend (it consisted of a sequence of random patterns) until the brief (500-ms) pulse of contrast modulation.
These results show that the peak stimulus activations do not co-localize with aFST, whereas the effects of SC inactivation do, indicating that the effect of SC inactivation in aFST and the behavioral deficits following inactivation of aFST cannot be attributed to stimulus blindness.

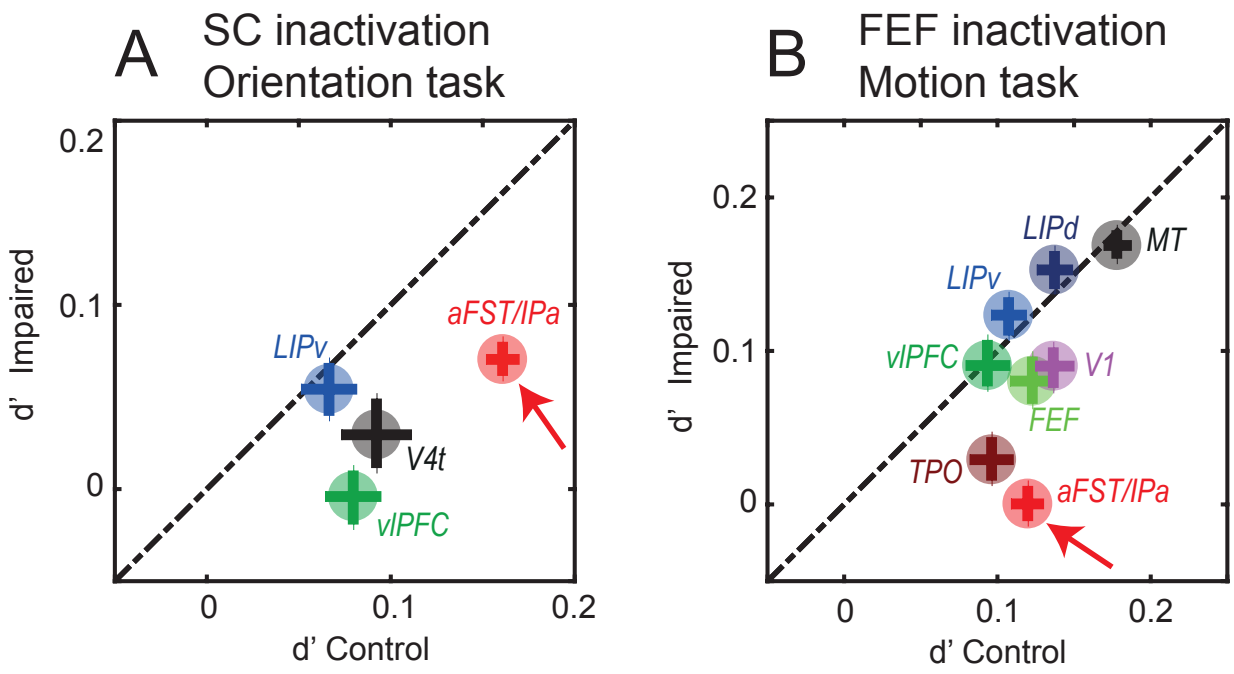

Figure S7. Comparison of the effects of impaired performance on the attention-related modulations in different cortical ROIs (related to Figures 5 and 6).

(**A**) Attention-related modulation during SC inactivation is plotted against attention-related modulation during control sessions for each significant ROI in the ipsilateral hemisphere of monkey #1 for the second-order orientation pulse task. The largest reduction was observed in region aFST/IPa (red arrow).

(**B**) Attention-related modulation for each significant ROI in the ipsilateral hemisphere of monkey #2 during impairments induced by reversible inactivation of the FEF, during the motion-change detection task. Again, the largest reduction was observed in region aFST/IPa (red arrow).